

ORIGINAL RESEARCH



CS1-specific single-domain antibodies labeled with Actinium-225 prolong survival and increase CD8⁺ T cells and PD-L1 expression in Multiple Myeloma

Kim De Veirman^a, Janik Puttemans^b, Ahmet Krasniqi^b, Thomas Ertveldt^c, Heleen Hanssens^b, Ema Romao^d, Dirk Hose^a, Cleo Goyvaert^c, Philip Vlummens^g, Serge Muyldermans^d, Karine Breckpot^c, Frank Bruchertseifer^f, Alfred Morgenstern^f, Matthias D'Huyvetter^{b*}, and Nick Devoogdt^{b*}

^aDepartment of Hematology and Immunology, Vrije Universiteit Brussel, Brussels, Belgium; ^bDepartment of Medical Imaging, Laboratory for in Vivo Cellular and Molecular Imaging, Vrije Universiteit Brussel, Brussels, Belgium; ^cLaboratory for Molecular and Cellular Therapy, Vrije Universiteit Brussel, Brussels, Belgium; ^dDepartment of Cellular and Molecular Immunology, Vrije Universiteit Brussel, Brussels, Belgium; ^eDepartment of Clinical Hematology, Ghent University Hospital, Ghent, Belgium; ^fEuropean Commission, Joint Research Centre (JRC), Karlsruhe, Germany

ABSTRACT

Multiple myeloma (MM) is a hematological malignancy characterized by the presence of clonal plasma cells in the bone marrow niche. Despite significant therapeutic advances, MM remains incurable for the majority of patients. Targeted radionuclide therapy (TRNT) has emerged as a promising treatment option to eradicate residual cancer cells. In this study, we developed and characterized single-domain antibodies (sdAbs) against the MM-antigen CS1 and evaluated its therapeutic potential in MM using TRNT. We first validated CS1 as potential target for TRNT. CS1 is expressed in normal and malignant plasma cells in different disease stages including progression and relapse. It is expressed in dormant as well as proliferating MM cells, while low expression could be observed in environmental cells. Biodistribution studies demonstrated the specific uptake of anti-CS1 sdAbs in tissues of 5TMM cell infiltration including bone, spleen and liver. TRNT using anti-CS1 sdAbs labeled with actinium-225 significantly prolonged survival of syngeneic, immunocompetent 5T33MM mice. In addition, we observed an increase in CD8⁺ T-cells and more overall PD-L1 expression on immune and non-immune cells, implying an interferon gamma signature using actinium-225 labeled CS1-directed sdAbs. In this proof-of-principle study, we highlight, for the first time, the therapeutic potential and immunomodulating effects of anti-CS1 radionuclide therapy to target residual MM cells.

ARTICLE HISTORY

Received 20 July 2021
Revised 27 October 2021
Accepted 27 October 2021

KEYWORDS

Multiple Myeloma; targeted radionuclide therapy; single domain antibody; CS1

Introduction

Multiple myeloma (MM) is a hematological malignancy characterized by the accumulation of malignant plasma cells in the bone marrow, leading to osteolytic lesions, cytopenia, anemia, and renal failure. First-line treatment of MM patients consists of a triple or quadruple combination of proteasome inhibitors (e.g. bortezomib), immunomodulatory drugs (e.g. lenalidomide) dexamethasone and monoclonal antibodies. In eligible patients, this treatment is followed by high-dose melphalan treatment and autologous stem cell transplantation.^{1,2} Immunotherapy with monoclonal or bispecific antibodies offers a non-cross resistant mechanism of action.^{3,4} Monoclonal antibodies (moAbs) specifically bind to antigens expressed on tumor cells triggering antibody dependent cell-mediated toxicity and complement-dependent cytotoxicity. Bispecific antibodies concomitantly bind a tumor-antigen and a target on immune cells (e.g. CD3 on T-cells). Several MM surface antigens are used as targets.⁴ Daratumumab or isatuximab (directed against CD38), elotuzumab (directed against CS1) and the antibody drug conjugate belantamab mafodotin (targeting BCMA) are approved for the treatment of MM.^{3,5}

T-cell bispecific antibodies in development include CC-93269 (BCMA-CD3 trivalent), teclistamab (BCMA-CD3) and talquetamab (GPCR5D-CD3).⁶ Despite therapeutic advances, MM remains incurable for the majority of patients due to the selection of unresponsive, drug-resistant tumor cells, making relapse imminent.

Coupling of antibodies or antibody fragments to powerful radionuclides, also called targeted radionuclide therapy (TRNT), is a promising therapeutic strategy with a non-cross resistant mechanism of action, even in the setting of chemoresistant clones and an exhausted immune system.⁷ One major limitation is the long blood half-life of moAbs, which leads to prolonged exposure to radioactivity in blood and highly perfused organs. As a result, myelotoxicity is a well-known consequence and dose limiting factor of TRNT. This could be especially a problem in heavily pretreated patients. Up till now, only two agents are FDA approved for commercial use, the radiolabeled anti-CD20 moAb ⁹⁰Y-ibritumomab and ¹³¹I-tositumomab to treat B cell non-Hodgkin lymphoma.^{8,9} In contrast to conventional antibodies that exist in all

CONTACT Kim De Veirman  kim.de.veirman@vub.be  Department of Hematology and Immunology, Vrije Universiteit Brussel, Laarbeeklaan 103, 1090 Brussels, Belgium

*Authors contributed equally

 Supplemental data for this article can be accessed on the [publisher's website](#)

© 2021 The Author(s). Published with license by Taylor & Francis Group, LLC.

This is an Open Access article distributed under the terms of the Creative Commons Attribution-NonCommercial License (<http://creativecommons.org/licenses/by-nc/4.0/>), which permits unrestricted non-commercial use, distribution, and reproduction in any medium, provided the original work is properly cited.

mammals, animals of the Camelidae family have antibodies that lack light chains and are solely composed of two identical heavy chains.¹⁰ Their variable domain can easily be produced in bacteria or yeast in large quantities with full retention of antigen-binding capacity, and is called a single-domain antibody (sdAb). sdAbs have superior biochemical characteristics including high stability, solubility, and target affinity. In addition, they are low immunogenic, can recognize epitopes that are undetectable for conventional antibodies and can be manipulated by genetic engineering.^{11,12} Because of their low molecular weight (15 kDa), sdAbs can efficiently penetrate dense tissues to deliver radionuclides. Moreover, unbound sdAb is rapidly removed from the body through the renal route limiting side effects.¹³ The past years, promising preclinical results were obtained with TRNT in MM. While the path of β^- particles can range from 1 to 10 millimeters and exert a bystander effect on neighboring healthy cells, α particles have a short path length (50–80 μm) and a high linear energy transfer (LET). Given their short range of energy deposition, α particles are considered ideal candidates to treat residual tumor cells.¹⁴

For TRNT, it is important to select molecular targets that are highly and selectively expressed on cancer cells. CS1 (SLAMF7) is a cell surface glycoprotein of the signaling lymphocyte activation molecule receptor family that is highly expressed on normal plasma cells and MM cells, with lower expression on natural killer (NK) cells and T-cells, and no expression on other normal tissues.¹⁵ The aim of our study was to specifically target MM cells *in vivo*, at a stage of low tumor burden, using CS1-targeting sdAbs radiolabeled with α -particle emitting actinium-225 (²²⁵Ac). The therapeutic efficacy and immunological effects were assessed in the 5T33MM model, an immunocompetent mouse model, which is characterized by the localization of MM cells in the bone marrow, the presence of a serum M component, increased angiogenesis and induction of osteolytic bone lesions; thereby faithfully replicating the human disease.^{16,17}

Materials and methods

5TMM mice and murine cell line

C57BL6 (Charles river) and C57BL/KalwRij mice (Envigo, Horst, Netherlands) were maintained following conditions approved by the Ethical Committee for Animal Experiments of VUB (license no. LA1230281, ECD17-281-11). The 5T33MM model originated from spontaneously developed MM in elderly C57BL/KalwRij mice and was propagated by intravenous transfer of the diseased marrow into young syngeneic mice.¹⁶

The 5T33MMvt and 5TGM1 GFP⁺ cells are *in vitro* variants of the 5T33MM cells and can grow stroma independently in RPMI1640 medium (Lonza) containing 10% fetal calf serum (Biocrom AG) and 5% supplements (penicillin/streptomycin, glutamine, and Na-pyruvate) at 37°C in a humidified atmosphere with 5% CO₂. For *in vivo* experiments, mice were intravenously inoculated with 5×10^5 5T33MM cells or 1×10^6 5TGM1 cells. The 5TGM1 cell line was previously engineered to express eGFP and was used to investigate

in vivo myeloma cell dormancy.¹⁸ Briefly, 5TGM1 GFP⁺ cells were labeled with the Vybrant® DID membrane dye (Eugene, Oregon, USA) and using flow cytometry proliferating (GFP⁺, DiD^{low/negative}) and dormant MM cells (GFP⁺, DiD⁺) could be distinguished.

Flow cytometry of CS1 expression in 5TGM1 and 5T33MM model

Total bone marrow and spleen cells were collected from diseased mice, followed by red blood cell lysis to analyze CS1 expression in murine samples. The following antibodies were used: CD3-PECy7 (clone 17A2, Cat# 100219), NK1.1-APCCy7 (clone PK136, Cat# 108723), CS1-PE (clone 4G2, Cat# 152005) (all derived from Biolegend) and *in house* purified 3H2 idiotype (secondary step: APC-labeled anti-mouse IgG1, clone RMG1-1, Cat# 406609, Biolegend). Cells were incubated for 30 min with the required antibodies (1/100 dilution) at 4°C. After washing, the percentage of positive cells and the mean fluorescence intensity (MFI) was measured using a FACSCanto Flow Cytometer (BD Biosciences) and analyzed with FlowJo 7 software (Tree Star Inc.).

MM patient cohorts

CS1 gene expression was investigated by the use of microarray data of the Heidelberg–Montpellier (HM) cohort (333 samples) and TT2 cohort (423 samples) using the Genomicscape webtool (accession number E-TABM-937, GSE2658).^{19,20} Gene expression data were normalized with the MAS5 algorithm. The Multiple Myeloma Research Foundation (MMRF) cohort (CoMMpass trial, IA14) was included to compare CS1 expression in pairs of newly diagnosed ($n = 40$) and relapsed patients ($n = 39$) (accessed in March 2020). Normalized transcripts per million (TPM) gene expression values, generated using RNA-sequencing, were downloaded alongside clinical data through the MMRF research portal (<https://research.themmr.org>).

CS1-specific sdAb generation, production and purification

A llama was immunized with recombinant mouse and human CS1 protein (U Protein Express) and injected once per week with 100 μg of recombinant protein with GERBU adjuvant LQ3000 (GERBU Biotechnik) for 6 weeks.^{21,22} Four days after the last injection, peripheral blood lymphocytes were extracted from 100 mL blood for sdAb library construction, as described earlier.^{21,23} Briefly, total mRNA was extracted from about 10^7 lymphocytes and 40 μg of mRNA was used to synthesize the cDNA. sdAb fragments were amplified using nested PCR and cloned in the pMECS phagemid using the golden gate assembly method. Resulting phagemids were electroporated into competent *E. Coli* TG1 cells. The capacity of the constructed library was measured by the number of colonies after serial dilution. Phages were enriched by four rounds of biopannings in solution using biotinylated CS1 protein and streptavidin beads. sdAb-containing periplasmic extracts (PEs) of randomly picked clones were screened by ELISA for binding to mouse CS1 protein and positive hits were sequenced. PEs were

additionally tested by flow cytometry. DNA fragments encoding for selected sdAbs were recloned in *E. Coli* WK6 expression vectors pHEN21 and pHEN6 that encode for untagged and His₆-tagged variants respectively. A non-targeting sdAb, R3B23, was used as a negative control in all experiments.²⁴ sdAb expression was induced overnight at 28°C with 1 mmol/L isopropylb-D-thiogalactoside. PEs were obtained by osmotic shock and further purified using immobilized metal affinity chromatography on His-Select Nickel Affinity Gel or on protein A Sepharose beads (for sdAb1) (both from Sigma), for His₆-tagged or untagged variants, respectively. The sdAbs were finally gel-filtrated using Superdex 75 16/60 columns (GE Healthcare Biosciences) in PBS.

Flow cytometry CS1-specific sdAb

In vitro binding of sdAbs was evaluated on 5T33MMv cells using flow cytometry. Briefly, 5×10^5 5T33MMv cells were incubated with 1 µg of His₆-tagged sdAb for 1 hour at 4°C. After washing the cells, sdAb binding was detected by sequential incubations with 1 µg anti-His mouse IgG1 antibody (clone AD1.1.10, Cat# MCA1396, AbD Serotec) and 1/100 APC-coupled anti-mouse IgG1 antibody (clone RMG1-1, Cat# 406609, Biolegend) for 30 min at 4°C. After washing, mean fluorescence intensity (MFI) was measured using a FACSCanto Flow Cytometer (BD Biosciences) and analyzed with Flow Jo 7 software (Tree Star Inc.).

Biacore

Binding affinity of sdAbs was analyzed via surface plasmon resonance (SPR) on a Biacore T200 device (Cytiva). mCS1-His was immobilized on a CM5 sensor chip. Binding studies were performed in HBS (20 mM of HEPES pH 7.4, 150 mM of NaCl, 0.005% Tween-20, and 3.4 mM of EDTA) as running buffer containing serial sdAb dilutions (500 to 1 nM, diluted 1/3) at a flow rate of 30 µL/min at 25°C. Between each flow cycle, the sensor chip was regenerated during 20 s with 100 mM Glycine-HCl (pH 2.5) at a flow rate of 30 µL/min. Curves were fitted using Biacore's evaluation software using a two-state reaction model to retrieve equilibrium dissociation constants (KD). The curve-fitting efficiency was evaluated by chi-square.

Biodistribution experiments and SPECT/CT imaging

Anti-mCS1 and R3B23 sdAbs were radiolabeled with Technetium-99m (^{99m}Tc) for biodistribution studies. ^{99m}Tc was incorporated at their His₆-tag via tricarbonyl chemistry and radiolabeled sdAbs were separated from unbound [^{99m}Tc]Tc(H₂O)₃(CO)₃⁺ via NAP-5 size-exclusion chromatography (SEC; Sephadex, GE Healthcare).^{23,25} The eluate was filtered and the radiochemical purity was evaluated by instant thin-layer chromatography (iTLC) on silica gel-impregnated glass fiber sheets (Agilent Technologies) before and after purification using acetone (Sigma) as mobile phase.

Naïve C57BL/KaLwRij, 5T33MM (19–21 days post-injection (d.p.i.), >80% tumor load) and 5TGM1 mice (27 d.p.i., 40–60% tumor load) were intravenously injected with ^{99m}Tc-sdAbs (injected activity 30–70 MBq, n = 3/sdAb). One hour post-

injection (1 h.p.i.), mice were imaged using pinhole SPECT/micro-CT with a Vector⁺/CT MILabs system. After imaging, mice were sacrificed and organs were isolated to evaluate the organ-specific uptake of the tracer using a γ-counter (Cobra Inspector 5003, Canberra, Packard, Illinois, IL, USA). The tissue/organ uptake was corrected for decay and calculated as the percentage of injected activity per gram tissue (%IA/g). Image analysis was performed using Medical Image Data Examiner (AMIDE) software,²⁶ and maximum intensity projections (MIPs) were generated using OsiriX Lite software.²⁷

TRNT experiments

The bifunctional chelator *p*-SCN-Bn-DOTA was purchased from Macrocylics. The bifunctional chelators were conjugated to lysines present in the protein sequence of the untagged sdAb. The conjugation reaction was performed in sodium carbonate buffer (0.05 mol/L, pH 8.2–8.5). The sdAbs were incubated with a 20-fold molar excess of the bifunctional chelator for 2 h at room temperature. The conjugate was purified by SEC using a Superdex Peptide 10/300 GL column (GE Healthcare).

Actinium-225 (²²⁵Ac) was obtained from JRC (Karlsruhe, Germany). The desired activity of [²²⁵Ac]AcCl₃ (1.8 – 2.2 MBq) was added to 100–120 µg of DOTA–sdAb conjugate in ammonium acetate buffer (0.5 mol/L, pH 5.2). The mixture was incubated for 90 min at 55°C while shaking. After cooling, 10 µL of 50 mM DTPA was added to complex unreacted radioisotopes. Purification of radiolabeled sdAbs was performed via NAP-5 SEC (GE Healthcare) with 0.1% Tween – 5 mg/mL ascorbic acid in PBS and filtered through a 0.22-mm filter (Millex). Radiochemical purity was evaluated using iTLC with citrate buffer (0.1 mol/L, pH4.0) used as mobile phase. [²²⁵Ac]Ac-DOTA-sdAb will be further referred to as [²²⁵Ac]-sdAb. A dosimetry experiment was performed in naïve C57BL/6 mice (Charles River). Mice were intravenously injected with 48.2 ± 2.5 kBq [²²⁵Ac]-sdAb (5.0 µg sdAb), co-administered with 150 mg/kg of the plasma expander Gelofusin.^{28,29} Mice were killed at 1, 24, 48 and 96 h.p.i. (n = 3/timepoint). Organs and tissues were isolated, weighed, counted, and expressed as %IA/g. The biodistribution data were time-integrated to calculate the residence time of radiolabeled sdAb per gram organ. The final 2 points were fitted to an exponential function to estimate the residence time to infinity. For each data set, the absorbed doses were obtained by multiplying the obtained residence time (radioactivity over time) with the corresponding S value for a 1 g sphere for ²²⁵Ac. The S value for ²²⁵Ac of 4.40×10^{-12} J.Bq⁻¹.s⁻¹ was obtained from RADAR phantoms (www.doseinfo-radar.com/RADARphan.html).

To assess the anti-tumor effects of [²²⁵Ac]-mCS1 sdAb, C57BL/KalwRij mice were intravenously inoculated with 5×10^5 5T33MM cells. At day 4, at a stage of low tumor burden (undetectable M protein by serum electrophoresis), mice were treated with four intravenous injections of saline buffer (control group), [²²⁵Ac]-R3B23 sdAb (50.2 ± 2.4 kBq/injection, control group) and [²²⁵Ac]-mCS1 sdAb (47.2 ± 3.1 kBq/injection) at day 4, 7, 10 and 13. [²²⁵Ac]-sdAbs were co-administered with 150 mg/kg Gelofusin (Braun Medical, Diegem, Belgium). For the survival

experiment ($n = 13/\text{group}$), mice were euthanized when weight loss exceeded 20%, or at the advent of paralysis of the hind limbs.

To assess immunological effects, mice ($n = 3/\text{group}$) were euthanized at day 18 (with 50% mortality in the buffer-treated group) and bone marrow was isolated followed by red blood cell lysis. The following antibodies were used to assess immunological effects by flow cytometry: Fixable Viability Dye eFluor™ 506 (Cat# 65-0866-14, ThermoFisher Scientific), CD45.2-APC-eF780 (clone 104, Cat# 560694, BD Biosciences), CD11b-AF700 (clone M1/70, Cat# 557960, BD Biosciences), CD4-AF700 (clone RM4-5, Cat# 561025, BD Biosciences), CD8a-BV450 (clone 53-67, Cat# 561109, BD Biosciences), F4/80-BV421 (clone 6F12, Cat# 746070, BD Biosciences), CD11c-BV650 (clone HL3, Cat# 564079, BD Biosciences), Ly6G-APC (clone 1A8, Cat# 560599, BD Biosciences), PD-L1-BV421 (clone MIH5, Cat# 564716, BD Biosciences).

Statistical analysis

For statistical analysis and survival analysis, Mann-Whitney U test and Log-rank (Mantel-Cox) tests were performed. $P < .05$ (*), $P < .01$ (**), and $P < .001$ (***) and $P < .0001$ (****) were considered statistically significant. Results are given as mean \pm standard deviation (SD).

Results

CS1 expression in MM patient samples and the 5TMM model

CS1 expression was analyzed in various cell populations of MM patients using the HM cohort including bone marrow stromal cells (BMSC), monocytic myeloid cells (CD14^+), granulocytic myeloid cells (CD15^+), CD3^+ T-cells, naive B-cells, MGUS, and primary MM cells (Figure 1a). A high CS1 expression could be observed in CD138^+ plasma cells

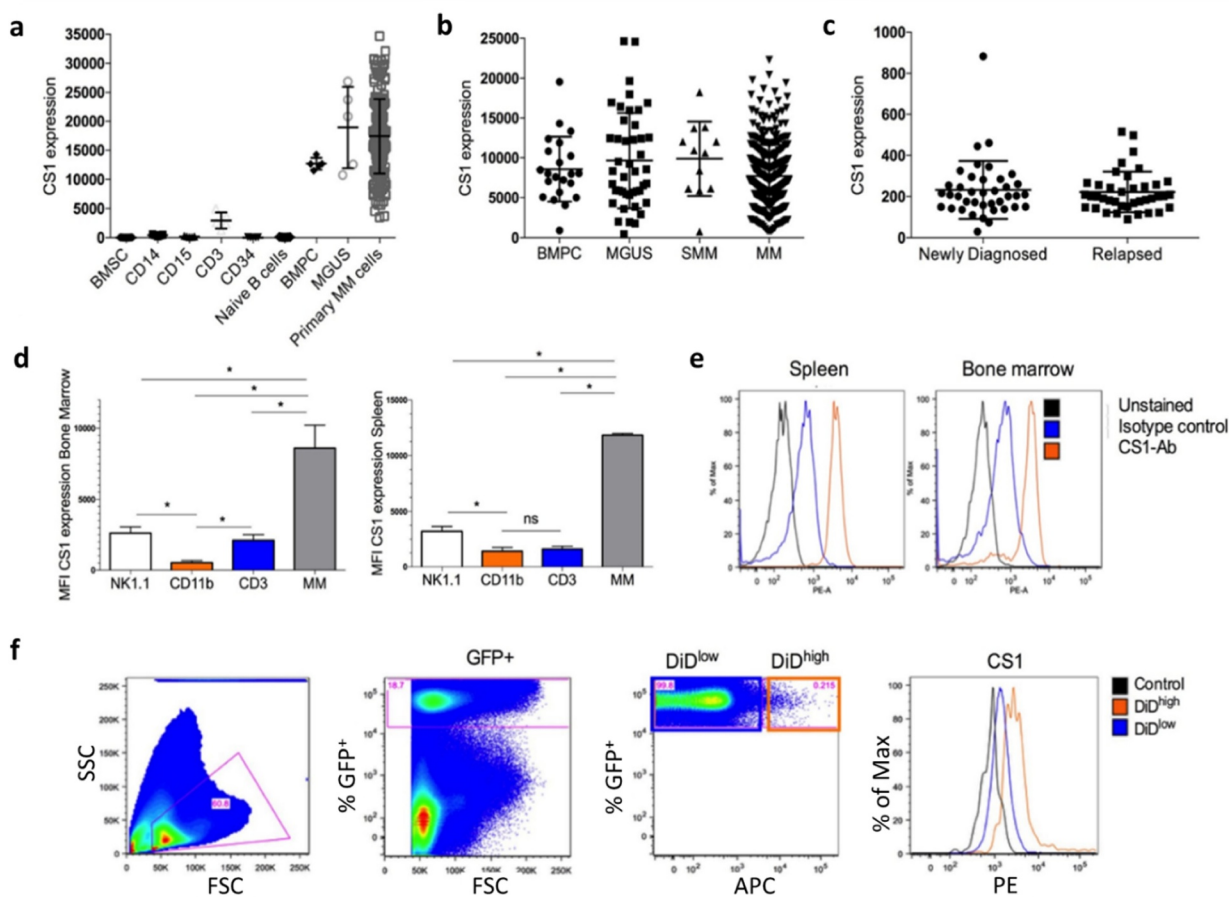


Figure 1. CS1 expression in MM patient samples and the 5TMM model. (a) CS1 expression was investigated using microarray data of the Heidelberg–Montpellier (HM) cohort. Expression was analyzed in bone marrow stromal cells (BMSC; $n = 5$), CD14^+ ($n = 5$), CD15^+ ($n = 5$), CD3^+ ($n = 5$), CD34^+ ($n = 5$), naive B-cells ($n = 5$), CD138^+ cells of patients with monoclonal gammopathy of undetermined significance (MGUS; $n = 5$) and primary MM cells of newly diagnosed patients ($n = 206$). (b) Using the TT2 cohort, CS1 expression was evaluated in bone marrow plasma cells (BMPC) from healthy donors ($n = 22$) and at various stages of MM disease including MGUS ($n = 44$), smoldering MM (SMM) ($n = 12$) and MM ($n = 345$). (c) CS1 expression in MM cells derived from newly diagnosed patients ($n = 40$) and at relapse ($n = 39$) (MMRF cohort). (d) CS1 expression in NK (idiotype⁻, NK1.1^+), myeloid (idiotype⁻, CD11b^+), T (idiotype⁻, CD3^+) and MM cells (idiotype⁺) derived from the bone marrow and spleen of the 5T33MM mouse model ($n = 3$, mean \pm SD, * $p < .05$, Mann-Whitney U test). (e) Representative flow cytometry result of CS1 expression in 5T33MM cells derived from spleen and bone marrow. (f) CS1 expression in proliferating and dormant MM cells using the *in vivo* 5TGM1 myeloma dormancy model. Dormant (5TGM1-GFP⁺, DiD^+) cells and proliferating (5TGM1-GFP⁺, DiD^-) myeloma cells were analyzed for CS1 expression by flow cytometry ($n = 3$, one representative result is shown).

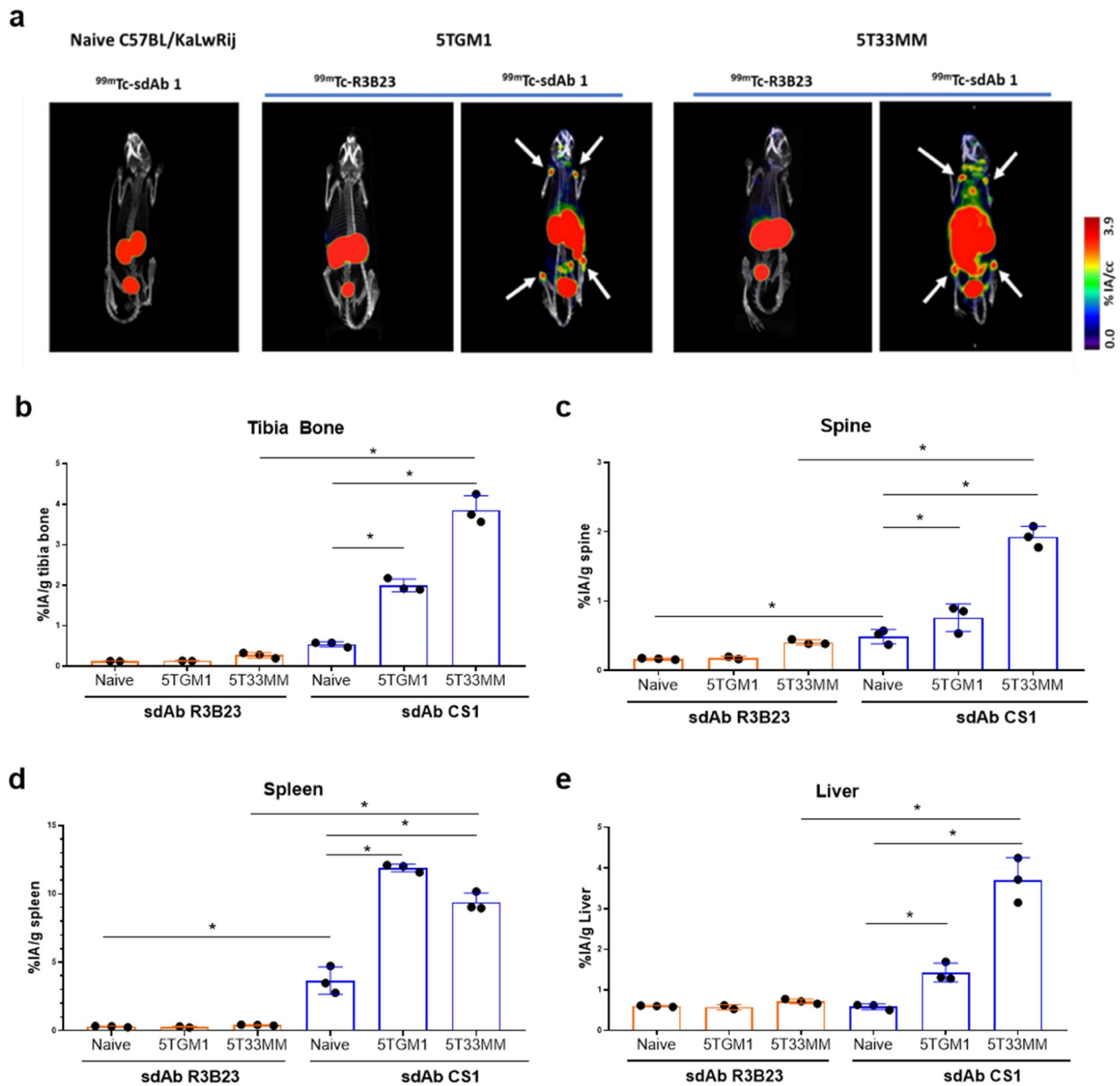


Figure 3. Biodistribution of CS1-specific sdAbs in naive, 5TGM1 and 5T33MM mice. (a) μ SPECT/CT images 1 h.p.i. of ^{99m}Tc -labeled sdAb1 in naive mice, 5TGM1 (moderate model) and 5T33 (aggressive model) MM mice. One representative picture ($n = 3/\text{sdAb}/\text{model}$). White arrows indicate bone uptake. (b-e) Organs were dissected and radioactivity was measured in bone, spine, spleen and liver ($n = 3/\text{sdAb}$). Data is presented as mean \pm SD percentage injected activity per gram organ or tissue (%IA/g). * $p < .05$, Mann-Whitney U test.

Biodistribution of CS1-specific sdAbs in naive, 5TGM1 and 5T33MM mice

Biodistribution of selected anti-mCS1 sdAbs was studied in naive mice (10 sdAbs, $n = 3/\text{sdAb}$), 5T33MM mice (10 sdAbs, $n = 3/\text{sdAb}$) and 5TGM1 mice (6 sdAbs, $n = 3/\text{sdAb}$) to monitor specific uptake in healthy and tumor-bearing organs including bone, spleen, and liver.¹⁶ sdAbs were radiolabeled with ^{99m}Tc and radiochemical purity was above 95%. One hour p.i., mice were subjected to full-body SPECT/CT scan, sacrificed and organs were collected to measure *ex vivo* radioactive uptake. Analysis of SPECT/CT images revealed that in healthy mice, differences between anti-mCS1 and control sdAb were minor, confirming the limited expression of mCS1 on normal cells (Figure 3a). High

signals were found for all sdAbs in the kidney and bladder, indicating a fast clearance of radiolabeled anti-mCS1 sdAbs (Supplementary Figure 1 and 2). In tumor-bearing mice, at end-stage of disease, sdAb1 showed the most elevated uptake in bone (tibia and spine), spleen and other MM-infiltrated organs, including liver compared to naive mice and control R3B23 sdAb (Figure 3b-e, supplementary Figure 1 and 2). Based on these results, anti-mCS1 sdAb1 was selected as a lead compound for further experiments: it binds *in vitro* to CS1 expressed on MM cells (Figure 2b), has an affinity of 25 nM (Figure 2c), a thermostability of 63°C (Figure 2d), shows lowest kidney retention (suppl Figure 1) and efficiently targets MM lesions *in vivo* in both bone and extramedullary regions (Figure 3).

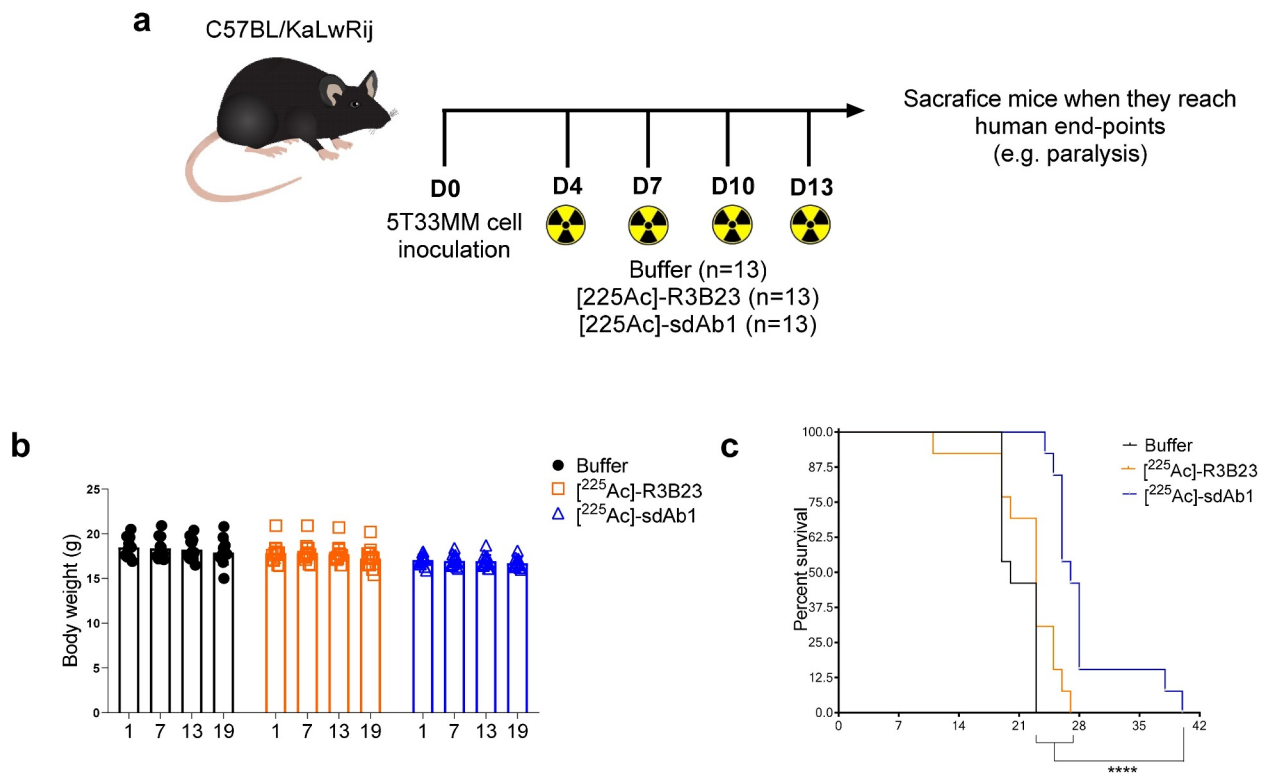


Figure 4. Anti-CS1 TRNT, in a stage of low tumor burden, significantly impacts the survival of 5T33MM mice. (a) Treatment schedule of 5T33MM mice with [²²⁵Ac]-sdAb1. Mice (n = 13/group) were treated with either saline buffer, [²²⁵Ac]-R3B23 sdAb (control sdAb) or [²²⁵Ac]-sdAb1 at day 4, 7, 10 and 13. At end-stage of disease, mice were sacrificed. (b) Body weight after α -TRNT with [²²⁵Ac]-sdAb1 in the 5T33MM model. (c) Survival curves after α -TRNT with [²²⁵Ac]-sdAb1 in the 5T33MM model. *p* values were determined using the log-rank test and found to be highly significant, *****p* < .0001.

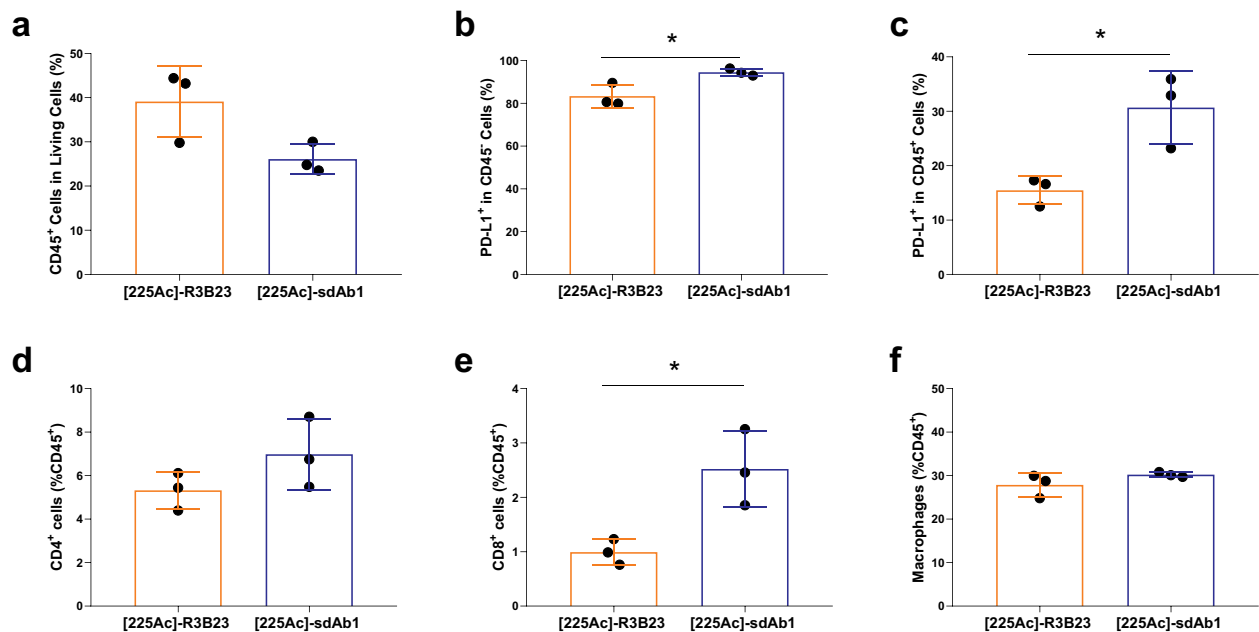


Figure 5. Anti-CS1 TRNT increased CD8⁺ T-cells and PD-L1 expression in the bone marrow of 5T33MM mice. 5T33MM mice (n = 3/group) were treated with either [²²⁵Ac]-R3B23 sdAb (control sdAb) or [²²⁵Ac]-sdAb1 at day 4, 7, 10 and 13. At day 18, mice were sacrificed and bone marrow cells were analyzed by flow cytometry. (a) % eF506⁻, CD45⁺ cells, (b) % PD-L1⁺ cells in CD45⁻ cells, (c) % PD-L1⁺ cells in CD45⁺ cells, (d) % CD8⁺ cells in CD45⁻ cells, (e) % CD4⁺ cells in CD45⁻ cells, (f) % CD11b⁺, CD11c⁻, Ly6G⁻, F4/80⁺ cells in CD45⁺ cells. Data is presented as mean \pm SD. **p* < .05, Mann-Whitney U test.

Dose finding and therapeutic efficacy of [²²⁵Ac]-mCS1 sdAb1 in MM

Tag-less sdAb1 was produced and purified, as the absence of tags was previously demonstrated to further reduce kidney retention.²⁹ To define the dose of [²²⁵Ac]-mCS1 sdAb1, a dosimetry experiment was performed in naive C57BL/6 mice. Pure [²²⁵Ac]-sdAbs were obtained with radiochemical yields of >50%, and radiochemical purities of >95% as determined by iTLC. Uptake in different organs/tissues was measured 1, 24, 48, and 96 h.p.i. The organ-absorbed doses for 1 kBq [²²⁵Ac]-sdAb1 are summarized in Supplementary Table 1. Kidneys received the highest absorbed dose of 0.755 Gy (1 h.p.i.).

The therapeutic potential of [²²⁵Ac]-sdAb1 was studied in the 5T33MM model (Figure 4a). As α -particle emitters are considered particularly suited to eliminate residual cancer cells, mice were treated at a stage of low tumor burden (4 days p.i.). At that time point, serum M protein cannot be detected by means of serum electrophoresis and the tumor load in the bone marrow and spleen is below 5%.³¹ Body weight did not significantly change between all groups (Figure 4b). No significant difference could be observed between the 5T33MM mice treated with either buffer or [²²⁵Ac]-R3B23 sdAb (median survival 20 and 23 days respectively). However, treatment with [²²⁵Ac]-sdAb1 significantly prolonged survival of 5T33MM mice compared to control groups (median survival of 27 days, 2 mice survived for 38 and 40 days, respectively, $p < .0001$) (Figure 4c).

Immunomodulating effects of [²²⁵Ac]-mCS1 sdAb1 in MM

To evaluate the immunological effects of α -particle TRNT, 5T33MM mice were treated as illustrated in Figure 4a and were all euthanized at day 18 (50% mortality in the buffer-treated group) to assess the percentage of different immune subsets in the bone marrow and spleen by flow cytometry. The gating strategy is provided in the supplementary Information (Supplementary Figure 3(a-b)). We observed a significant increase in PD-L1 expression, in both immune cells (CD45⁺) and non-immune cells (CD45⁻), in the bone marrow of mice treated with [²²⁵Ac]-sdAb1 compared to [²²⁵Ac]-R3B23 (Figure 5(a-c)). Furthermore, the percentage of T-cells was significantly increased, more specifically the percentage of CD8⁺ T-cells upon treatment with [²²⁵Ac]-sdAb1 (Figure 5d). No difference could be observed in the percentage of CD4⁺ T-cells and macrophages in the bone marrow treated with either [²²⁵Ac]-R3B23 or [²²⁵Ac]-sdAb1 (Figure 5(e-f)). In the spleen, a significant increase in CD45⁺ cells, PD-L1 expression and CD8⁺ T-cells could be observed as well (Supplementary Figure 4S(a-e)).

Discussion

TRNT is an attractive approach to eliminate residual MM cells, which is not cross-resistant with chemotherapy or other therapeutic agents. Besides DNA damage, TRNT might reshape the immunological tumor microenvironment by induction of immunogenic cell death and/or type I interferons, stimulating both the innate and adaptive immune response. Moreover,

recent data suggest that other cell compartments beyond the cell nucleus play an important role in the fate of irradiated cells. Communication between irradiated cells and neighboring cells over a short distance (bystander) and longer distance (immune activation) contribute to non-targeted effects that play an important role in the efficacy of TRNT.^{32–34} Recent studies demonstrated the therapeutic potential of radioimmunotherapy with anti-CD38, anti-CD138 and anti-idiotypic in preclinical MM models.^{24,35–37} In this study, we aimed to target MM cells using radiolabeled CS1-specific sdAbs.

It has been shown that CS1 is highly expressed on healthy and malignant plasma cells. In addition, CS1 was detected in 95% of the MM patients, independent of their cytogenetic abnormalities.¹⁵ Using different MM patient cohorts, we could confirm high CS1 expression in normal and malignant plasma cells, at diagnosis and relapse. Consistent with previous studies,^{15,38} we observed a low expression of CS1 in NK cells and T-cells of 5T33MM mice. A low expression of a target antigen also on T-cells does not exclude compound activity as shown by CD20-directed radioimmunotherapeutics (e.g. ⁹⁰Yttrium ibritumomab tiuxetan, FDA approved), which have a favorable toxicity profile in B-cell lymphoma despite the expression of CD20 on B-cells and a subset of T-cells.³⁹ Dormant MM cells, which reside in specific niches within the marrow and are considered a basis of disease relapse, also expressed high levels of CS1, indicating that CS1 is an attractive candidate to eliminate residual MM cells.

To specifically target CS1 expressing MM cells using a TRNT approach, we preferred the use of camelid derived sdAbs. These sdAbs combine the beneficial properties of small molecules and monoclonal antibodies, which makes them suitable agents for radioimmunotherapeutic approaches.^{13,40} We generated a library of anti-CS1 sdAbs from which sdAb1 was selected as the lead compound based on its optimal characteristics, particularly its cell binding and *in vivo* tumor targeting potential. We observed a clear accumulation in spleen, liver, and bone of tumor-bearing mice compared to healthy mice. The 5TMM models have similar characteristics as the human disease including the secretion of M protein and the localization of malignant plasma cells in the marrow.¹⁶ However, it is known that 5T33 and 5TGM1 cells home to spleen and livers as well, which explains the specific uptake of sdAb1 in these organs. In tumor-free mice, we also found a higher uptake of sdAb1 in lungs, spleen, lymph nodes and bone compared to control sdAb R3B23; potentially associated with the targeting of immune cells in these tissues. A similar biodistribution profile of anti-mCD38 antibodies has been observed as well, which demonstrated a high accumulation in spleen, liver, and lungs of naive mice.⁴¹

Especially in the context of residual disease, α -particle emitters have important advantages over β^- particle emitters including their short range in tissue (50–80 μ m) and increased killing efficiency due to high linear energy transfer.¹⁴ Minnix et al. demonstrated superior effects of anti-CD38 antibodies radiolabeled with α -particle emitter ²²⁵Ac compared to β^- particle emitter ¹⁷⁷Lu in delaying tumor growth and decreasing whole-body toxicity.³⁵ In this study, we radiolabeled CS1-specific sdAb1 with ²²⁵Ac to investigate the impact on overall survival. Dosimetry experiments revealed that kidneys were the dose-

limiting organ (0.775 Gy/kBq), which is attributed to the renal accumulation of small peptides and proteins. Mice were treated at a stage of low tumor burden (day 4 – day 13, <5% tumor cells in bone marrow and spleen), to mimic a residual disease setting in MM patients. We observed a significant increase in overall survival of 5T33MM mice treated with [²²⁵Ac]-sdAb1 compared to mice treated with [²²⁵Ac]-R3B23 sdAb. Further optimization of the dose and treatment schedule is required to improve the long-term efficacy of the therapy and prevent MM recurrence. In addition, exploring the effect of [225Ac]-sdAb1 on CS1 expression of residual tumor cells is warranted to investigate whether TRNT results in the outgrowth of a CS1-negative tumor subset.

In MM, it remains unclear how to best integrate TRNT with immunotherapy. Interestingly, we observed increased PD-L1 expression in immune and nonimmune cells upon [²²⁵Ac]-sdAb1 treatment, implying an interferon-gamma signature and immune activation. This is consistent with previous observations by Chen et al., who found that ¹⁷⁷Lu TRNT increased PD-L1 expression in T-cells and that PD-1/PD-L1 blockade combined with TRNT improved overall survival in a murine colon cancer model.⁴² A recent study by Patel et al. also demonstrated the immunomodulating potential of TRNT in a manner that promotes the response to immune checkpoint inhibitors.⁴³ TRNT (⁹⁰Y-NM600) combined with anti-CTLA4 treatment resulted in production of pro-inflammatory cytokines, expansion of CD8⁺ T cells and significantly improved survival in mice bearing 4T1 breast tumors and B78 melanoma tumors.⁴³ In addition, Jagodinsky et al. demonstrated a STING-dependent type I interferon activation in melanomas, head and neck cancer murine models following TRNT.³³ Despite the expression of CS1 on T-cells, we did not observe any detrimental effect on the T cell population, in contrast we found a significant increase in the percentage CD8⁺ T-cells after TRNT. All these data point to the immune-stimulating properties of TRNT and its therapeutic potential in combination with current immunotherapeutic approaches including immune checkpoint inhibitors. However, the functionality of T-cells (e.g. interferon-gamma secretion, cytotoxic effects) and the potential effects on healthy cells (e.g. normal plasma cells, NK cells) need to be investigated in future studies.

In conclusion, this study demonstrated the potential of CS1 as a target, expressed by proliferating and dormant MM cells. Administration of [²²⁵Ac]-sdAb1 significantly impacted the survival of tumor-bearing mice, highlighting its potential as a new therapeutic approach for MM patients. Moreover, this study provides supportive data to combine TRNT and other immunotherapeutic approaches; and offers a promising new treatment modality for MM patients.

Acknowledgments

The authors thank Charlotte Van De Walle, Carine Seynaeve, Cindy Peleman, Jan De Jonge and Kevin de Jonghe for their technical assistance. Data of the CoMMpass trial (IA14) were generated as part of the Multiple

Myeloma Research Foundation Personalized Medicine Initiatives (<https://research.themmr.org> and www.themmr.org)”.

Disclosure statement

M.D. and N.D. are respectively employee and consultant of Precirix NV and hold ownership interest (including patents) in sdAb radiodiagnostics and radiotherapeutics. All other authors have declared no conflicts of interest. The funders had no role in the design of the study; in the collection, analyses, or interpretation of data; in the writing of the manuscript, or in the decision to publish the results.

Funding

This study was supported by Fonds Stimulans, International Myeloma Foundation (IMF), VUB spearhead research programs, Stichting tegen Kanker (number 2016-076; FAF-F/2016/798) and infrastructure and research funding from Research Foundation-Flanders (Fonds Wetenschappelijk Onderzoek, FWO) (I001618N, 1502018N, 1501920N, and G028220N). H.H., J.P., and T.E. received a personal predoctoral mandate from FWO-SB (1S55621N, 1S27716N, 1S06622N). M.D. and K. D.V. are postdoctoral fellows of FWO (12H3619N, 12I0921N).

ORCID

Philip Vlummens  <http://orcid.org/0000-0001-8275-2887>

Highlights:

- CS1 is highly expressed on MM cells, while low expression could be observed on environmental cells of the bone marrow.
- High levels of CS1 could be detected on dormant and proliferating MM cells.
- CS1-directed targeted radionuclide therapy significantly increased CD8⁺ T-cells and PD-L1 expression.
- CS1-directed targeted radionuclide therapy significantly prolonged survival *in vivo*.

Author contributions

Conception and design: K. De Veirman, M. D’Huyvetter, N. Devoogdt; Development of methodology: K. De Veirman, M. D’Huyvetter, N. Devoogdt; Acquisition of data: K. De Veirman, N. Devoogdt, J. Puttemans, A. Krasniqi, H. Hanssens, E. Romao, C. Goyvaert, T. Ertveldt; Analysis and interpretation of data: K. De Veirman, A. Krasniqi, J. Puttemans, D. Hose, T. Ertveldt, P. Vlummens, N. Devoogdt; Writing, review, and/or revision of the manuscript: K. De Veirman, J. Puttemans, A. Krasniqi, H. Hanssens, E. Romao, D. Hose, P. Vlummens, S. Muyltermans, K. Breckpot, F. Bruchertseifer, A. Morgenstern, M. D’Huyvetter, N. Devoogdt; Material support: F. Bruchertseifer, A. Morgenstern; Study supervision: K. De Veirman, M. D’Huyvetter, N. Devoogdt.

References

1. Gandolfi S, Prada CP, Richardson PG. How I treat the young patient with multiple myeloma. *Blood*. 2018;132(11):1114–1124. doi:10.1182/blood-2017-05-693606.
2. Gulla A, Anderson KC. Multiple myeloma: the (r)evolution of current therapy and a glance into the future. *Haematologica*. 2020;105:2358–2367. doi:10.3324/haematol.2020.247015.
3. Radocha J, van de Donk NWCJ, Weisel K. Monoclonal antibodies and antibody drug conjugates in multiple myeloma. *Cancers (Basel)*. 2021;13:1–24. doi:10.3390/cancers13071571.

4. Verkleij CPM, Bruins WSC, Zweegman S, van de Donk NWCJ. Immunotherapy with antibodies in Multiple Myeloma: monoclonals. Bispecifics Immunoconjugates Hemato. 2021;2:116–130.
5. Nooka AK, Weisel K, Van De Donk NWCJ, Routledge D, Otero PR, Song K, Quach H, Callander N, Minnema MC, Trudel S, et al. Belantamab mafodotin in combination with novel agents in relapsed/refractory multiple myeloma: DREAMM-5 study design. *Future Oncol.* 1987–2003;17:2021.
6. Barilà G, Rizzi R, Zambello R, Musto P. Drug conjugated and bispecific antibodies for multiple myeloma: improving immunotherapies off the shelf. *Pharmaceuticals.* 2021;14(1):1–19. doi:10.3390/ph14010040.
7. Sgouros G, Bodei L, McDevitt MR, Nedrow JR. Radiopharmaceutical therapy in cancer: clinical advances and challenges. *Nat Rev Drug Discov.* 2020;19:589–608.
8. Wahl RL. Tositumomab and 131I therapy in non-Hodgkin's lymphoma. *J Nucl Med.* 2005;46:128–140.
9. Ferrucci PF, Vanazzi A, Grana CM, Cremonesi M, Bartolomei M, Chinol M, Ferrari M, Radice D, Papi S, Martinelli G, et al. High activity 90Y-ibritumomab tiuxetan (Zevalin®) with peripheral blood progenitor cells support in patients with refractory/resistant B-cell non-Hodgkin lymphomas. *Br J Haematol.* 2007;139:590–599. doi:10.1111/j.1365-2141.2007.06869.x.
10. Jovčevska I, Muylldermans S. The Therapeutic Potential of Nanobodies. *BioDrugs.* 2020;34(1):11–26. doi:10.1007/s40259-019-00392-z.
11. Ackaert C, Smiejewska N, Xavier C, Sterckx YGJ, Denies S, Stijlemans B, Elkrim Y, Devoogdt N, Caveliers V, Lahoutte T, et al. Immunogenicity Risk Profile of Nanobodies. *Front Immunol.* 2021;12:632687. doi:10.3389/fimmu.2021.632687.
12. Muylldermans S. Nanobodies: natural single-domain antibodies. *Annu Rev Biochem.* 2013;82:775–797. doi:10.1146/annurev-biochem-063011-092449.
13. D'Huyvetter M, Xavier C, Caveliers V, Lahoutte T, Muylldermans S, Devoogdt N. Radiolabeled nanobodies as theranostic tools in targeted radionuclide therapy of cancer. *Expert Opin Drug Deliv.* 2014;11:1939–1954. doi:10.1517/17425247.2014.941803.
14. Dekempeneer Y, Keyaerts M, Krasniqi A, Puttemans J, Muylldermans S, Lahoutte T, D'huyvetter M, Devoogdt N. Targeted alpha therapy using short-lived alpha-particles and the promise of nanobodies as targeting vehicle. *Expert Opin Biol Ther.* 2016;16:1035–1047. doi:10.1080/14712598.2016.1185412.
15. Hsi ED, Steinle R, Balasa B, Szmania S, Draksharapu A, Shum BP, Huseni M, Powers D, Nanisetti A, Zhang Y, et al. CS1, a potential new therapeutic antibody target for the treatment of multiple myeloma. *Clin Cancer Res.* 2008;14:2775–2784. doi:10.1158/1078-0432.CCR-07-4246.
16. Vanderkerken K, Asosingh K, Croucher P, Van Camp B. Multiple myeloma biology: lessons from the 5TMM models. *Immunol Rev.* 2003;194:196–206. doi:10.1034/j.1600-065X.2003.00035.x.
17. Vlummens P, De Veirman K, Menu E, De Bruyne E, Offner F, Vanderkerken K, Maes K. The use of murine models for studying mechanistic insights of genomic instability in multiple myeloma. *Front Genet.* 2019;10:1–11. doi:10.3389/fgene.2019.00740.
18. Lawson MA, McDonald MM, Kovacic N, Khoo WH, Terry RL, Down J, Kaplan W, Paton-Hough J, Fellows C, Pettitt JA, et al. Osteoclasts control reactivation of dormant myeloma cells by remodelling the endosteal niche. *Nat Commun.* 2015;6:1–15. doi:10.1038/ncomms9983.
19. Kassambara A, Rème T, Jourdan M, Fest T, Hose D, Tarte K, Klein B. GenomicScape: an easy-to-use web tool for gene expression data analysis. application to investigate the molecular events in the differentiation of B cells into plasma cells. *PLoS Comput Biol.* 2015;11:1–10. doi:10.1371/journal.pcbi.1004077.
20. Moreaux J, Hose D, Kassambara A, Rème T, Moine P, Requirand G, Goldschmidt H, Klein B. Osteoclast-gene expression profiling reveals osteoclast-derived CCR2 chemokines promoting myeloma cell migration. *Blood.* 2011;117:1280–1290. doi:10.1182/blood-2010-04-279760.
21. Pardon E, Laeremans T, Triest S, Rasmussen SGF, Wohlkönig A, Ruf A, Muylldermans S, Hol WGJ, Kobilka BK, Steyaert J. A general protocol for the generation of Nanobodies for structural biology. *Nat Protoc.* 2014;9:674–693. doi:10.1038/nprot.2014.039.
22. Arbabi Ghahroudi M, Desmyter A, Wyns L, Hamers R, Muylldermans S. Selection and identification of single domain antibody fragments from camel heavy-chain antibodies. *FEBS Lett.* 1997;414(3):521–6. doi: 10.1016/S0014-5793(97)01062-4.
23. Krasniqi A, D'Huyvetter M, Xavier C, Van Der Jeught K, Muylldermans S, Van Der Heyden J, Lahoutte T, Tavernier J, Devoogdt N. Theranostic radiolabeled anti-CD20 sdAb for targeted radionuclide therapy of non-hodgkin lymphoma. *Mol Cancer Ther.* 2017;16:2828–2839. doi:10.1158/1535-7163.MCT-17-0554.
24. Lemaire M, D'Huyvetter M, Lahoutte T, Van Valckenborgh E, Menu E, De Bruyne E, Kronenberger P, Wernery U, Muylldermans S, Devoogdt N, et al. Imaging and radioimmunotherapy of multiple myeloma with anti-idiotypic Nanobodies. *Leukemia.* 2014;28:444–447. doi:10.1038/leu.2013.292.
25. Xavier C, Devoogdt N, Hernot S, Vaneycken I, Huyvetter MD, De Vos J, Massa S, Lahoutte T, Caveliers V. Site-specific labeling of his-tagged Nanobodies with ^{99m}Tc: a practical guide. *Methods Mol Biol.* 2012;911:485–90. doi:10.1007/978-1-61779-968-6_30.
26. Loening AM, Gambhir SS. AMIDE: a free software tool for multi-modality medical image analysis. *Mol Imaging.* 2003;2:131–137. doi:10.1162/153535003322556877.
27. Rosset A, Spadola L, Ratib O. OsiriX: an open-source software for navigating in multidimensional DICOM images. *J Digit Imaging.* 2004;17:205–216. doi:10.1007/s10278-004-1014-6.
28. Dekempeneer Y, Caveliers V, Ooms M, Maertens D, Gysemans M, Lahoutte T, Xavier C, Lecocq Q, Maes K, Covens P, et al. Therapeutic efficacy of 213Bi-labeled sdAbs in a preclinical model of ovarian cancer. *Mol Pharm.* 2020;17:3553–3566. doi:10.1021/acs.molpharmaceut.0c00580.
29. D'Huyvetter M, Vincke C, Xavier C, Aerts A, Impens N, Baatout S, De Raeve H, Muylldermans S, Caveliers V, Devoogdt N, et al. Targeted radionuclide therapy with A 177Lu-labeled anti-HER2 nanobody. *Theranostics.* 2014;4:708–720. doi:10.7150/thno.8156.
30. Khoo WH, Ledergor G, Weiner A, Roden DL, Terry RL, McDonald MM, Chai RC, De Veirman K, Owen KL, Opperman KS, et al. A niche-dependent myeloid transcriptome signature defines dormant myeloma cells. *Blood.* 2019;134:30–43. doi:10.1182/blood.2018880930.
31. De Veirman K, van Ginderachter JA, Lub S, de Beule N, Thielemans K, Bautmans I, Oyajobi BO, De Bruyne E, Menu E, Lemaire M, et al. Multiple myeloma induces Mcl-1 expression and survival of myeloid-derived suppressor cells. *Oncotarget.* 2015;6:10532–10547. doi:10.18632/oncotarget.3300.
32. Sia J, Szmyd R, Hau E, Gee HE. Molecular Mechanisms of Radiation-Induced Cancer Cell Death: a Primer. *Front Cell Dev Biol.* 2020;8:1–8. doi:10.3389/fcell.2020.00041.
33. Jagodinsky JC, Jin WJ, Bates AM, Hernandez R, Grudzinski JJ, Marsh IR, Chakravarty I, Arthur IS, Zangl LM, Brown RJ, et al. Temporal analysis of type I interferon activation in tumor cells following external beam radiotherapy or targeted radionuclide therapy. *Theranostics.* 2021;11:6120–6137. doi:10.7150/thno.54881.
34. Pouget JP, Constanzo J. Revisiting the Radiobiology of Targeted Alpha Therapy. *Front Med.* 2021;8:1–11. doi:10.3389/fmed.2021.692436.

35. Minnix M, Adhikarla V, Caserta E, Poku E, Rockne R, Shively JE, Pichiorri F. Comparison of CD38-targeted α - versus β -radionuclide therapy of disseminated multiple myeloma in an animal model. *J Nucl Med.* 2021;62:795–801. doi:10.2967/jnumed.120.251983.
36. Fichou N, Gouard S, Maurel C, Barbet J, Ferrer L, Morgenstern A, Bruchertseifer F, Faivre-Chauvet A, Bigot-Corbel E, Davodeau F, et al. Single-dose anti-CD138 radioimmunotherapy: bismuth-213 is more efficient than lutetium-177 for treatment of multiple myeloma in a preclinical model. *Front Med.* 2015;2:76. doi:10.3389/fmed.2015.00076.
37. Puttemans J, Stijlemans B, Keyaerts M, Vander Meeren S, Renmans W, Fostier K, Debie P, Hanssens H, Rodak M, Pruszynski M, et al. The road to personalized myeloma medicine: patient-specific single-domain antibodies for anti-idiotypic radionuclide therapy. *Mol Cancer Ther.* 2021. doi:10.1158/1535-7163.MCT-21-0220.
38. Tai YT, Dillon M, Song W, Leiba M, Li XF, Burger P, Lee AI, Podar K, Hideshima T, Rice AG, et al. Anti-CS1 humanized monoclonal antibody HuLuc63 inhibits myeloma cell adhesion and induces antibody-dependent cellular cytotoxicity in the bone marrow milieu. *Blood.* 2008;112:1329–1337. doi:10.1182/blood-2007-08-107292.
39. Witzig TE, Gordon LI, Cabanillas F, Czuczman MS, Emmanouilides C, Joyce R, Pohlman BL, Bartlett NL, Wiseman GA, Padre N, et al. Randomized controlled trial of yttrium-90-labeled ibritumomab tiuxetan radioimmunotherapy versus rituximab immunotherapy for patients with relapsed or refractory low-grade, follicular, or transformed B-cell non-Hodgkin's lymphoma. *J Clin Oncol.* 2002;20:2453–2463. doi:10.1200/JCO.2002.11.076.
40. Lecocq Q, De Vlaeminck Y, Hanssens H, D'Huyvetter M, Raes G, Goyvaerts C, Keyaerts M, Devoogdt N, Breckpot K. Theranostics in immuno-oncology using nanobody derivatives. *Theranostics.* 2019;9:7772–7791. doi:10.7150/thno.34941.
41. Quelven I, Monteil J, Sage M, Saidi A, Mounier J, Bayout A, Garrier J, Cogne M, Durand-Panteix S. ^{212}Pb α -radioimmunotherapy targeting CD38 in multiple myeloma: a preclinical study. *J Nucl Med.* 2020;61:1058–1065. doi:10.2967/jnumed.119.239491.
42. Chen H, Zhao L, Fu K, Lin Q, Wen X, Jacobson O, Sun L, Wu H, Zhang X, Guo Z, et al. Integrin $\alpha\beta 3$ -targeted radionuclide therapy combined with immune checkpoint blockade immunotherapy synergistically enhances anti-tumor efficacy. *Theranostics.* 2019;9:7948–7960. doi:10.7150/thno.39203.
43. Patel RB, Hernandez R, Carlson P, Grudzinski J, Bates AM, Jagodinsky JC, Erbe A, Marsh IR, Arthur I, Aluicio-Sarduy E, et al. Low-dose targeted radionuclide therapy renders immunologically cold tumors responsive to immune checkpoint blockade. *Sci Transl Med.* 2021;13:1–18.